Angewandte Chemie
Eine Zeitschrift der Gesellschaft Deutscher Chemiker

Supporting Information

Suppression of SARS-CoV-2 Replication with Stabilized and Click-Chemistry Modified siRNAs

F. R. Traube, M. Stern, A. J. Tölke, M. Rudelius, E. Mejías-Pérez, N. Raddaoui, B. M. Kümmerer, C. Douat, F. Streshnev, M. Albanese, P. R. Wratil, Y. V. Gärtner, M. Nainytė, G. Giorgio, S. Michalakis, S. Schneider, H. Streeck, M. Müller, O. T. Keppler, T. Carell**

Methods

Design of siRNA sequences

siRNA sequences against the SARS-CoV-2 RNA genome and transcripts were designed based on the Wuhan reference genome (NC_045512) and https://cov-lineages.org/global_report_B.1.617.2.html using web-based tools, such as the siRNA-design tool from Eurofins (http://eurofinsgenomics.eu/en/ecom/tools/sirna-design/) and the RNAxs webserver (http://rna.tbi.univie.ac.at/cgi-bin/RNAxs/RNAxs.cgi).

Cloning of the luciferase reporter system

Synthetic target sequences (obtained from either *Eurofins, Genewiz* or *Thermo Scientific*), which are listed in Table S2, were cloned into psiCheck2 (*Promega* C8021) using the NEB HiFi Assembly Kit (*New England Biolabs*). Two approaches were tested: either reporter plasmid constructs into which the siRNA target sequences were directly placed next to each other (no viral sequence context) or reporter plasmid constructs in which the siRNA target sequences were kept in the original sequence context to reflect local RNA structure variations that might occur in the viral genome and impact on siRNA binding.

Synthesis and purification of RNA oligonucleotides

Unmodified RNA oligonucleotides (Table S1) were purchased from *Ella Biotech*. Modified RNA oligonucleotides (Table S5, Figure S5) were synthesized on a 1 µmol scale using an RNA automated synthesizer (*Applied Biosystems 394 DNA/RNA Synthesizer*) with standard phosphoramidite chemistry. Oligonucleotides were synthesized in DMT-OFF mode using DCA as a deblocking agent in CH_2Cl_2, BTT or Activator 42® as activator in MeCN, Ac_2O as capping reagent in pyridine/THF and I_2 as oxidizer in pyridine/H_2O. All canonical and modified phosphoramidites were obtained from *Linktech*, *Sigma-Aldrich* and *Baseclick*. The cleavage and deprotection of the CPG bound RNA oligonucleotides were performed with $NH_4OH_{(aq.)}$/$NH_2Me_{(aq.)}$ (1/1, 1 mL) at 65 °C for 5 min. The supernatant was transferred and the solution was evaporated at 35 °C under reduced pressure. The residue was subsequently heated with a solution of trimethylamine trihydrofluoride (98% in triethylamine, 125 µL) in DMSO (100 µL) at 65 °C for 1.5 h. Upon cooling in an ice bath, NaOAc (3.0 M, 25 µL) and *n*-BuOH (1 mL) were added. The resulting suspension was vortexed and cooled in a freezer (-80 °C) for 30 min. After the centrifugation, the supernatant was removed and the remaining oligonucleotide pellet was dried under vacuum. The oligonucleotides were further purified by semi-preparative reverse-phase HPLC using an *Agilent Technologies 1260 Infinity II* System with a *G7114A* detector equipped with the column *Nucleosil VP 250/10 C18* from *Macherey Nagel*. A gradient of 0-30% of buffer B in 45 min was applied (0-40% for highly modified strands). The buffer system: buffer A: 100 mM NEt_3/HOAc, pH 7.0 in H_2O and buffer B: 100 mM NEt_3/HOAc in 80% (v/v) acetonitrile. A flow rate of 5 mL/min was applied for the semi-preparative purifications. Analytical RP-HPLC was performed on an *Agilent Technologies 1260 Infinity II* System with a *G7114A* detector equipped with the column *Nucleosil 250/4 C18* from *Macherey Nagel* using a flow rate of 1 mL/min. The extinction coefficients were calculated using the software OligoAnalyzer (http://eu.idtdna.com/calc/analyzer) from *Integrated DNA-Technologies*. The structural integrity of the synthesized oligonucleotides was analysed by MALDI-TOF mass measurement using a 3-hydroxypicolinic acid matrix.

Synthesis and purification of peptide P

Commercially available reagents were used throughout without purification. Wang resin was purchased from *Sigma Aldrich*. *N*,*N*'-diisopropylethylamine (DIEA) was purchased from *Sigma-Aldrich*. *N*-Fmoc amino acids and (benzotriazol-1-yloxytripyrrolidinophosphonium hexafluorophosphate) (PyBOP) were purchased from *IRIS Biotech GMBH*. Solid phase synthesis (SPS) grade organic solvents (DMF, DCM) were used for solid peptide phase synthesis (SPPS) and were purchased from *Carlo Erba*. MilliQ water was used for RP-HPLC analyses and semi-preparative purifications. SPPS was performed automatically on a *Liberty Blue* peptide synthesizer (*vide infra*) (*CEM mWaves S.A.S., Germany*). RP-HPLC and ESI-HRMS analyses were carried out on a *LCMS Bruker MicroTOF II* equipped with a *Thermo Ultimate 3000* HPLC line using a *Phenomenex Kinetex EVO C18* column (50 mm × 2.1, 2.6 µm) at a flow rate of 0.5 mL/min. The mobile phase was composed of 0.1% (v/v) HCOOH-H_2O (Solvent A) and 0.1% HCOOH-CH_3CN (Solvent B). Detection was performed at three different wavelengths (200, 214 and 254 nm) and the column temperature in the oven was maintained at 50 °C. Semi-preparative purifications of peptides were performed on a *Thermo Ultimate 3000* using a *Macherey Nagel Nucleodur C18ec* column (250 × 10 mm, 5 µm) at a flow rate of 5 mL/min. The mobile phase was composed of 0.1% (v/v) TFA-H_2O (Solvent A) and 0.1% TFA-CH_3CN (Solvent B). Column eluent was monitored by UV detection at 214 and 254 nm. The purity of the compounds after purification was determined to be ≥ 95%.

P was prepared on a 100 µmol scale. Polystyrene Wang resin (loading 0.37 mmol/g) was placed in the reaction vessel, and pre-swollen with DMF for 1 h. Loading of *N*-Fmoc-Leu-OH (10 equiv. relative to the resin loading) on the resin was carried out manually by using the symmetrical anhydride pre-activation procedure in the presence of DIC (5 equiv.) in anhydrous DCM for 20 min and subsequent addition of the symmetrical anhydride to the resin in

the presence of DMAP (0.1 equiv.) in DMF at room temperature for 2 h. The resin was then filtered off and washed with DMF (3 × 3 mL). The vessel was then placed inside the microwave reactor of the *Liberty Blue*. Microwave irradiation was next applied during coupling and deprotection steps. The temperature was maintained by modulation of power and controlled with a fiber optic sensor. Fmoc removal was carried out with 20% of piperidine in DMF (2 x 3 mL) under microwave irradiation (75 °C, 100 W, 30 sec then 75 °C, 100 W, 180 sec). The resin was then filtered off and washed with DMF (3 x 3 mL). *N*-Fmoc-Xaa-OH (5 equiv. relative to the resin loading), PyBOP (5 equiv.) and DIEA (10 equiv.), were dissolved in DMF. The vessel was then irradiated (75 °C, 30 W, 300 sec). The resin was then filtered off and washed with DMF (3 x 3 mL). Each coupling step was repeated once. To note, Fmoc-Arg(Pbf)-OH (2 x 5 equiv.) was coupled by conventional method without microwave irradiation by using the same number of equivalents of coupling reagents for 1500 sec. The azido-Deg_3-acetic acid was at last introduced following the same coupling conditions to those applied for the Arg coupling. Finally, the resin was swollen in a mixture TFA/TIS/H_2O/ (95:2.5:2.5, v/v/v) and left to react for 4 h under slight shaking. The resin was filtered off, washed with TFA (2 x 2 mL) and the filtrate was precipitated in cold Et_2O. The crude oligomer was lyophilized then analysed by RP-HPLC before to be purified by preparative RP-HPLC using the appropriate gradient to a final purity ≥ 95%.

The desired peptide **P** (N_3-Deg_3-CO-Tyr-Lys-Tyr-Arg-Tyr-Leu-OH) was purified by preparative RP-HPLC (Figure S6A) with a gradient 20-44% of buffer B in 15 min at a flow rate of 5 mL/min.

ESI-MS (ESI+): m/z calculated for $C_{53}H_{77}N_{13}O_{14}$: 1120.5786 $[M+H]^+$ found 1120.5337 $[M+H]^+$ (Figure S6B).

Click procedure

The fluorophore dye azides were purchased from *Jena Bioscience* and *Baseclick*. To a solution of the oligonucleotide (4.0 mM in H_2O, 5.0 µL) an azide solution (20 mM in DMSO, 4.0 µL), $CuSO_4$ (50 mM in 100 mM THPTA solution in H_2O, 5.0 µL) and ascorbate (50 mM in H_2O, 10 µL) were added. The reaction mixture was degassed with argon and thoroughly shaken at 25 °C for 1 h. The crude mixtures were first purified by a *Bio-Gel P-6* column and subsequently by reversed-phase HPLC (Table S6). The click products were analysed by analytical reversed-phase HPLC and MALDI-TOF (Figure S7). For the peptide click triethylammonium acetate buffer (1.0 M in H_2O, 20 µL) and aminoguanidine hydrochloride (50 mM in H_2O, 4.0 µL) were additionally added.

siRNA hybridization

The annealing of the double strands was performed in the hybridization buffer (10 mM Tris-HCl (pH = 8), 1 mM EDTA, 50 mM NaCl) by heating to 95 °C for 2 min and cooling to 10 °C within 85 min (gradient -1 °C/min) using a *TAdvanced Twin* Thermocycler from *Biometra*.

Serum stability assay

Human serum (human male AB plasma, USA origin) was purchased from *Sigma Aldrich* and pre-heated at 37 °C before the RNA duplex (9/1, Serum/RNA) was added. At certain time points, samples (100 µL) were taken and extracted with phenol (300 µL) and ddH_2O (200 µL). After centrifugation for 3 min at 4 °C and 21000 x *g* the supernatant was collected in a separate Eppendorf tube. The step was repeated twice. The combined aqueous phases were washed three times with chloroform and centrifuged for 1 min at 4 °C. After filtration (0.2 µm) the volume was reduced to 150 µL under reduced pressure. The samples (75 µL) were analysed by analytical reversed-phase HPLC (Figure S8). Analytical reversed-phase HPLC was performed with a gradient of 0-20% (**S-6**), 0-25% (**S-6^{m}**) and 0-35% (**S-6^{fm}**) of buffer B in 60 min. The column oven was heated to 50 °C for the **S-6** strand.

Cell culture

Vero-E6 cells (American Type Culture Collection, ATCC, Virginia, USA), A549 cells (human lung carcinoma cell line; American Type Culture Collection, ATCC, Virginia, USA), Caco-2 cells (human colorectal adenocarcinoma cell line, ATCC, Virginia, USA) and MDA-MB-231 cells (triple-negative human breast adenocarcinoma; DSMZ-German Collection of Microorganisms and Cell Cultures GmbH, Braunschweig, Germany) were cultivated at 37 °C in a humidified incubator with atmospheric oxygen concentrations (21%) and 5% CO_2. The cells were maintained in Dulbecco's Modified Eagle's Medium (DMEM) high glucose containing 10% fetal bovine serum (FBS), 100 U/mL penicillin-streptomycin and NEAA (culture medium). Cells were routinely passaged when reaching a confluence of 80 - 90%.

Dual-luciferase assay

All quantities refer to the amounts required for one well. The activity of the prepared siRNAs was tested against different reporter plasmids (**A1** - **A3**) that either contained just the sequence of the leader sequence (**A1**) or a 350 bp long insert, which included multiple target sites in the respective sequence context of the viral genome (**A2**), or a concatenated sequence of multiple viral 21mer target sites (**A3**) (Figure S1b). For the dual-luciferase assay (Dual-

Glo Luciferase assay, *Promega*), 9500 A549 cells were plated in a 96 well microplate (*Greiner*) in 100 µL of culture medium. 24 h after seeding, the cells were transfected with 0.5 ng reporter plasmid using 0.25 µL of transfection reagent jetPRIME (*Polyplus Transfection VWR*) as described by the manufacturer. 2 – 3 h after plasmid transfection, the medium was exchanged, and siRNA transfection was performed using 2 pmol of siRNA (20 nM final concentration) and 0.25 µL of Lipofectamine RNAiMAX (*Thermo Fisher Scientific*) as described by the manufacturer. 24 h after siRNA transfection, the medium was exchanged to 70 µL of DMEM low glucose without phenol red containing 10% FBS and the assay was performed according to the manufacturer's manual on a Tecan Plate Reader (*Tecan GENios Pro*, luminescence mode). The assay was performed in technical quadruplicates. For the analysis, the *Renilla* luciferase signal was divided by the firefly luciferase signal of the same well. Afterwards, the mean of the *Renilla*/firefly luciferase ratios of the technical replicates was calculated and knockdown efficiencies were determined as described in the statistical analysis section.

siRNA delivery into Caco-2 cells

Caco-2 cells (3 x 10^4 per well) were plated in a µ-slide 8 well chamber (*ibidi*) in 200 µL RPMI-1640 containing 10% FBS. 30 h after seeding, 180 pmol of siRNA per well (900 nM final concentration) were added. 18 h post transfection, the cells were washed twice with HBSS (*Sigma Aldrich*). 16% FA (*Thermo Fisher Scientific*) was diluted in DPBS to reach a 4% working solution and cells were fixed for 10 min. Afterwards, cells were washed three times with DPBS, stained with Hoechst 33342 (5 µg/mL working solution) for 10 min. Then, cells were washed with DPBS and mounted using Fluoroshield histology mounting medium (*Sigma Aldrich*) prior to microscopy. Confocal microscopy was performed using a Leica SP8 confocal laser scanning microscope (*Leica*) with the associated LAS X software and Z-series spanning the full cell volume with a step size of 0.43 µm and a total size of 2.99 µm were acquired. Using *ImageJ*, final images that represent maximum intensity projections were calculated.

Isolation and expansion of SARS-CoV-2 clinical isolates

Replication-competent SARS-CoV-2 was expanded using waste material from PCR-positive nasopharyngeal swabs as reported[1] (PMID: 34379308; PMID: 34713795; PMID: 35090165). High-titer virus stocks were characterized by RT-qPCR, as reported previously[2], and the infectious titer was determined on human A549 cells and MDA-MB-231 cells, overexpressing the human angiotensin-converting enzyme 2 receptor, hACE2, referred to as A549-hACE2 cells and MDA-MB-231-hACE2 cells, respectively (see also "infection-induced cytotoxicity assay"). In parallel, for expanded stocks of SARS-CoV-2 near full-length genome sequences were generated following the ARTIC network nCoV-2019 sequencing protocol v2[3] as described previously[4].

RNA interference with SARS-CoV-2 in Vero-E6 cells

For siRNA transfection, 2 pmol siRNA and 0.25 µL Lipofectamine RNAiMAX were each mixed with 10 µL Opti-MEM (*Thermo Fisher Scientific*) per reaction. The two mixtures were combined and after an incubation of 20 min at room temperature, 100 µL of DMEM/10% FBS were added. For pre-infection treatment experiments, the resulting mixture was added to cells of a 96 well plate seeded the day before with 2 x 10^4 cells/well and incubated for 1 h at 37 °C. Thereafter, the siRNA mixture was removed, and cells were infected with SARS-CoV-2 (pangolin lineage B.3) at an MOI of 0.01 for 1 h at 37 °C. After removing the virus inoculum, cells were washed once with medium and incubated again with 120 µL DMEM/10% FBS. For post-infection treatment experiments, cells were infected first with SARS-CoV-2 at an MOI of 0.01. After infection for 1 h at 37 °C, cells were washed once with medium before the siRNA transfection was performed as described above. At 24 h post-infection, virus released into the supernatant was titered on Vero E6 cells by plaque assay using a methylcellulose overlay as described previously [5]. Additional details about the analysis are given in the statistical analysis section.

Infection-induced cytotoxicity assay

A549-hACE2 cells (1.5 x 10^4 cells per well) or MDA-MB-231-hACE2 cells (2.0 x 10^4 cells per well) were plated in a 96-well white well half area plate with clear bottom (*Corning*) in culture medium. At the indicated time points, target cells were treated with either siRNAs at indicated concentrations or RDV (1 µM) two hours before infection. Subsequently, cells were challenged with a serial dilution of a stock of the indicated SARS-CoV-2 clinical isolate. In all cases, infection was performed in "virus infection medium" (DMEM, 2% FBS, 100 U/mL penicillin-streptomycin, NEAA). 48 h (MDA-MB-231-hACE2 cells) or 72 h (A549-hACE2 cells) after infection, analysis of virus-induced killing of target cells was performed by measurement of viability of target cells using the CellTiter-Glo 2.0 reagent (*Promega*). Cells were treated according to the manufacturer's instructions. In brief, 15 µL CellTiter-Glo 2.0 reagent was added to each well, incubated for 10 min in the dark at room temperature and luminescence was recorded using the Infinite F200 microplate reader (*Tecan*). Viability of cells was calculated by normalization of readings for infected cells relative to those for untreated control cells.

RT-qPCR analysis of infection of A549-hACE2 cells with SARS-CoV-2
A549-hACE2 (3.0 x 10^4 cells per well) were plated in a 96-well plate (*Sarstedt*) in culture medium. Next, target cells were treated either 24 h before infection with siRNAs or 2 h before infection with RDV (1 µM). For infection, cells were challenged with a serial dilution of a SARS-CoV-2 B.1.177 (EU1) stock. In all cases, infection was performed in infection medium. 3 h post-infection, infection medium was removed, cells were washed once with PBS and fresh culture medium was added. A post wash sample was taken. 48 h post-infection, supernatants and cells were lysed using the MagnaPure lysis buffer (MagNA Pure LC Total Nucleic Acid Isolation Kit - Lysis/Binding Buffer Refill; *Roche*) and heat inactivated (65 °C for 15 min). Samples were analysed by RT-qPCR.

Virus-supernatant transfer assay
A549-hACE2 cells (1.25 x 10^5 cells per well) were plated in a 12-well plate (*Sarstedt*) in culture medium. Next, target cells were transfected with siRNAs (24 h before infection) using Lipofectamine RNAiMAX. The next day, transfection medium was replaced with virus infection medium. Treatment with RDV (1 µM) served as infection control. Subsequently, cells were challenged with the indicated volume of a SARS-CoV-2 B.1.177 (EU1) stock. 72 h after infection, supernatants were harvested, cleaned from cellular debris by centrifugation (600 x g, 10 min, room temperature), and either lysed using the MagnaPure lysis buffer (MagNA Pure LC Total Nucleic Acid Isolation Kit - Lysis/Binding Buffer Refill; *Roche*) followed by heat-inactivation (65 °C for 15 min), or used to infect new target cells. Samples were analysed by real-time RT-PCR. In parallel, MDA-MB-231-hACE2 cells (2.0 x 10^4 cells per well) were plated in a 96-well white well half area plate with clear bottom (*Corning*) in virus infection medium. Subsequently, cells were challenged with a serial dilution of the previously generated supernatants. 48 h after infection, analysis of virus-mediated killing of target cells was performed by measurement of viability of target cells using the CellTiter-Glo 2.0 reagent (*Promega*) as described in the viability assay section.

Infection of 3D lung microtissue with SARS-CoV-2
EpiAirway™ 3D tracheobronchial microtissues (*MatTek Life Sciences)* were cultivated according to the manufacturer's instructions. Culture medium was supplied by the manufacturer. In brief, upon arrival, tissues were placed in 12-well hangtop plates with 5 mL of pre-warmed medium. Medium was replaced the next day for better equilibration of tissues. 24 h later, tissues were transferred into 6-well plates and treated with the indicated concentrations of siRNAs. The next day, siRNA-containing medium was removed and replaced with fresh medium. Treatment with RDV (10 µM) served as infection control. Subsequently, tissues were challenged with SARS-CoV-2 (B.1.177 8EU1). 3 h after infection, virus infection medium was removed, and tissues were washed twice with PBS from both the basal and apical side. An apical post-wash sample was taken for further analysis. Next, fresh medium was added. 72 h after infection, an apical wash was performed and stored, and both apical wash and tissues were lysed using the MagnaPure lysis buffer (MagNA Pure LC Total Nucleic Acid Isolation Kit - Lysis/Binding Buffer Refill; *Roche*) followed by heat inactivation (65 °C for 15 min). Samples were analysed by RT-qPCR.

Viral RNA isolation and cDNA synthesis
Viral nucleic acid extraction of inactivated cell culture supernatants was done using the Beckmann Biomek NX robotics platform (*Beckmann Coulter*) and the RNAdvance Viral (*Beckmann Coulter*) according to manufacturer's instructions. Subsequently, cDNA synthesis was performed using the High-Capacity RNA-to-cDNA (*Thermo Fisher Scientific*) according to manufacturer's instructions. cDNA synthesis was performed for 60 min at 37 °C, 5 min at 95° C on a PCR cycler (*Eppendorf*).

RT-qPCR (*N*, *RdRp* and *E* gene)
Allplex™ 2019-nCoV Assay *(Seegene Germany*) was used to detect SARS-CoV-2 RNA according to the manufacturer's instructions. In brief, 17 µl of reaction mix were added to 8 µL of nucleic acid eluate. Samples were measured in 96-well plates using the *Bio-Rad* CFX96 Dx System (C1000 Thermal Cycler). Data was analysed using the Seegene 2019-nCoV Viewer (ver 3.18.005.003).

RT-qPCR (*S* gene)
2 µL of cDNA product was amplified using iTaq Universal SYBR Green Supermix (*Bio-Rad*) on a qTOWER³/G cycler (*Jena Biosciences*). qPCR primers (Spike-total) are reported in Table S7.

RT-qPCR (SARS-CoV-2 sgmRNAs)
RT-qPCR was performed using either SARS-CoV-2 forward primer leader universal (600 nM) in combination with a gene-specific sgmRNA reverse primer (600 nM), or GAPDH forward and reverse primers (600 nM each), see Table S7. Quantification of sgmRNAs and GAPDH was done in a standard PowerUp SYBR Green PCR on a QuantStudio 3 Real-Time PCR System (*Thermo Fisher Scientific*).

RNA FISH and quantification of apoptosis in SARS-CoV-2 infected EpiAirway™

1.5 µm slides of formalin-fixed and paraffin embedded (FFPE) organoids were stained with hematoxylin and eosin (*H&E*). All slides were evaluated by an experienced pathologist (MR) and apoptosis was quantified in 10 high-power fields (HPFs) per organoid.

For *in situ* hybridization SARS-CoV-2-spike probe (RNAscope CoV2019-S-antisense; *ACD Bio-Techne*) was validated on FFPE SARS-CoV-2 infected and uninfected Caco-2 cells. 1.5 µm sections of FFPE organoids were processed according to the manufacturer´s protocol. Detection was carried out with OPAL 570 (*Akoya Bioscience*). Slides were scanned using a Vectra Polaris™ imaging system (*Akoya Bioscience*) and 10 region of interest (ROIs) were chosen for quantification using HALO software.

Statistical analysis and reproducibility

Statistical analysis for all experiments was performed using Graphpad Prism (8.0.0 or newer).

Figure 1b Data from two (**S-7**) to three (**L-1**, **R-2** to **R-5**, **S-6**, **S-8**, **S-9**) biologically independent experiments are displayed. Reduction of *Renilla* luciferase was calculated using equation (I). $Targeting_{siRNA}$ is one of the siRNAs **L-2**, **R-2** to **R-5** or **S-6** to **S-9**.

$$Renilla\ reduction\ (\%) = 100 - 100 \cdot \frac{Ratio_{\frac{Renilla}{Firefly}}(Targeting_{siRNA})}{Ratio_{\frac{Renilla}{Firefly}}(Ctrl.-10)}\ (I)$$

Figure 1c, d Data from three to five replicates from in total two independent experiments are displayed. Reduction of PFU/mL was calculated for each replicate using equation (II). $Targeting_{siRNA}$ is one of the siRNAs **L-2**, **R-2** to **R-5** or **S-6** to **S-9**.

$$Reduction\frac{PFU}{mL}\ (\%) = 100 - 100 \cdot \frac{Targeting_{siRNA}}{Ctrl.-10}\ (II)$$

Figure 1f – h Representative data from one out of two independent experiments are displayed. Graphs show mean of two technical replicates from one independent experiment.

Figure 1i Data from one independent experiment are displayed. Graphs show mean of two technical replicates from this experiment.

Figure 1f – i CV50 was calculated using [Inhibitor] vs normalized response – Variable slope [2] with the equation (III). Details about the CV50 are listed in Table S3.

$$Y = \frac{100}{1 + \frac{X^{HillSlope}}{CV50^{HillSlope}}}\ (III)$$

Figure 2b Data from four to five independent experiments are displayed. Ordinary one-way ANOVA (p-value < 0.0001) combined with Dunnett's multiple comparisons test (Alpha 0.05) was performed with **S-6** as the control column. Adjusted p-values for Dunnett's multiple comparisons test: **S-6** vs. **S-6^{hm}** <0.0001, **S-6** vs **S-6^{m}** 0.9974.

Figure 2c, d Representative data from one out of two independent experiments are displayed.

Figure 2e – f Representative data from one out of three independent experiments are displayed. Graphs show mean of two technical replicates. CV50 was calculated using [Inhibitor] vs normalized response – Variable slope [2] with the equation (III). Details about the CV50 are listed in Table S4. The values for IC50 (= mean), Std. Error IC50 (= SEM) and Degrees of Freedom +1 (= n) were grouped (columns: treatment, rows: siRNA concentration) and multiple unpaired t-tests (one per row, individual variance for each row, multiple comparisons adjustment using FDR (Q 1%) two-stage set-up method by Benjamini, Krieger and Yetkutieli) q value for t-tests: 20 nM **S-6^{m}** vs. **S-6** 0.032105, 2 nM **S-6^{m}** vs. **S-6** 0.000707, 0.2 nM **S-6^{m}** vs. **S-6** < 0.000001, 0.02 nM **S-6^{m}** vs. **S-6** 0.010881**.**

Figure 3b Representative images of one out of three independent experiments are displayed.

Figure 3c Graphs represent data of two independent tissue batches and each batch included one to three independent wells. Data of all independent wells were considered for the analysis. C_t values for untreated, 10 µM RDV and 300 nM **S-6^m-P** were grouped (columns: treatment, rows: fraction) and ordinary two-way ANOVA (p-value interaction 0.0214, p-value treatment 0.0008, p-value fraction <0.0001) combined with Dunnett's multiple comparisons test (Alpha 0.05) was performed to compare within each fraction (row) the different treatments (column) compared to the untreated control. Adjusted p-values for Dunnett's multiple comparisons test: untreated vs. **S-6^m-P** 0.4923 (post-wash), 0.0070 (apical wash harvest), 0.0040 (tissue harvest); untreated vs. RDV 0.8760 (post-wash), 0.0088 (apical wash harvest), 0.0006 (tissue harvest).

Figure 3d Graphs represent data of two independent tissue batches and each batch included one to three independent wells. Data of all independent wells were considered for the analysis. C_t values for untreated, 10 µM RDV and 300 nM **S-6^m-P** were grouped (columns: treatment, rows: gene) and ordinary two-way ANOVA (p-value interaction 0.2116, p-value treatment <0.0001, p-value gene <0.0001) combined with Dunnett's multiple comparisons test (Alpha 0.05) was performed to compare within each gene (row) the different treatments (column) compared to the untreated control. Adjusted p-values for Dunnett's multiple comparisons test: untreated vs. **S-6^m-P** 0.0062 (N), 0.0154 (S), 0.0167 (M), 0.0278 (E), 0.9780 (GAPDH); untreated vs. RDV 0.0024 (N), 0.0006 (S), 0.003 (M), 0.0015 (E), 0.9517 (GAPDH).

Figure 3e Representative images of one out of three independent experiments are displayed.

Figure 3f Quantification was performed for each condition in three independent tissue batches, one independent well per condition per batch. Quantification was done for ten independent HPFs per well. Data were entered in a nested table with three main columns (untreated, 300 nM **S-6^m-P**, 10 µM RDV) and each main column had three sub-columns (one sub-column per independent tissue). Nested one-way ANOVA (p-value <0.0001) combined with Dunnett's multiple comparisons test (Alpha 0.05) was performed to compare results of **S-6^m-P** and RDV treated tissues to untreated tissues. Adjusted p-value untreated vs. **S-6^m-P** <0.0001, untreated vs. RDV < 0.0001.

Figure 3g Representative images of one out of three independent experiments are displayed. Graph shows data from three independent tissue batches. Quantification of apoptosis in untreated, **S-6^m-P** and RDV treated tissues was analysed using ordinary one-way ANOVA (p-value 0.0002) combined with Dunnett's multiple comparisons test (Alpha 0.05) to compare apoptosis between untreated and **S-6^m-P** or RDV-treated tissues. Adjusted p-values for Dunnett's multiple comparisons test: untreated vs. S**-6^m-P** 0.0004, untreated vs. RDV 0.0002.

Figure 4a – c, e Representative data of one out of two independent experiments are shown.

Figure S4d Graphs represent data of one independent tissue batch, which included two to three independent wells. Data of all independent wells were considered for the analysis. C_t values for uninfected, untreated, 10 µM RDV, 300 nM **S-6^m-P** and 300 nM **Ctrl.-10^m-P** were grouped (columns: treatment, rows: gene) and ordinary two-way ANOVA excluding the uninfected samples (p-value interaction 0.0096, p-value treatment 0.0002, p-value fraction <0.0001) combined with Tukey's multiple comparisons test (Alpha 0.05) was performed to compare within fraction (row) the different treatments (column) among each other. Adjusted p-values for Tukey's multiple comparisons test for untreated vs. **S-6^m-P** 0.8425 (Post-Wash), 0.0010 (Apical Wash), 0.0032 (Tissue) and **Ctrl.-10^m-P** vs. **S-6^m-P** 0.7612 (Post-Wash), 0.0032 (Apical Wash), 0.0301 (Tissue)

Supplementary Figures

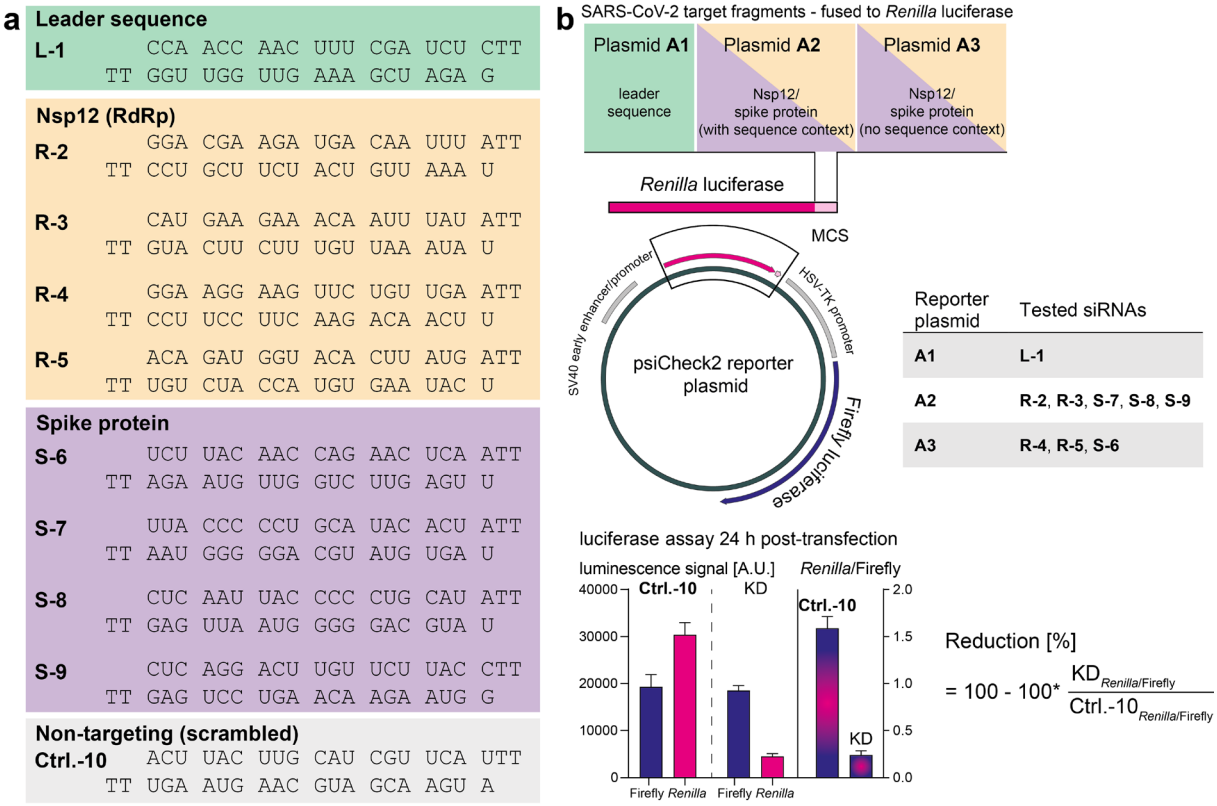

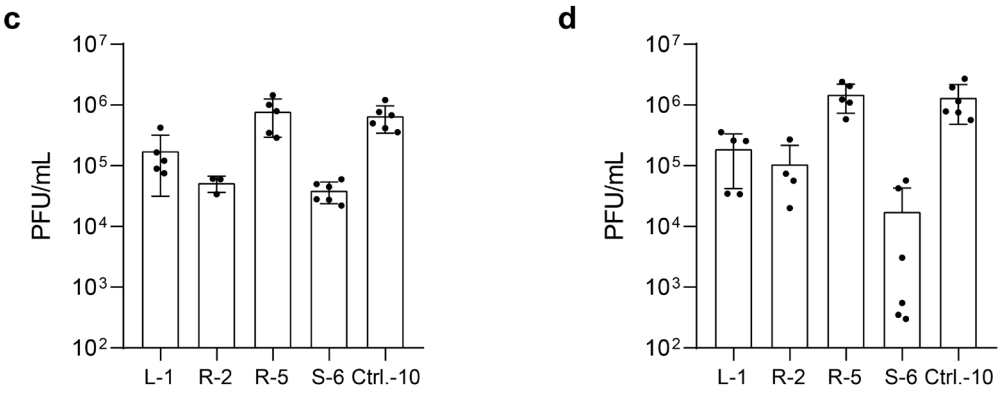

Figure S1: siRNA sequences, dual-luciferase reporter assay and antiviral activity in Vero-E6 cells. (a) Sequences of the designed siRNA duplexes. (b) Reporter plasmids for the dual-luciferase reporter assay and analysis of the assay to screen siRNA efficiency. (c, d) PFU/mL in Vero-E6 cells 72 h post SARS-CoV-2 infection (MOI 0.01). Cells were treated with 17 nM of the respective siRNAs (lipofection) either 1 h before (c) or 1 h after virus challenge (d). PFU = plaque forming units.

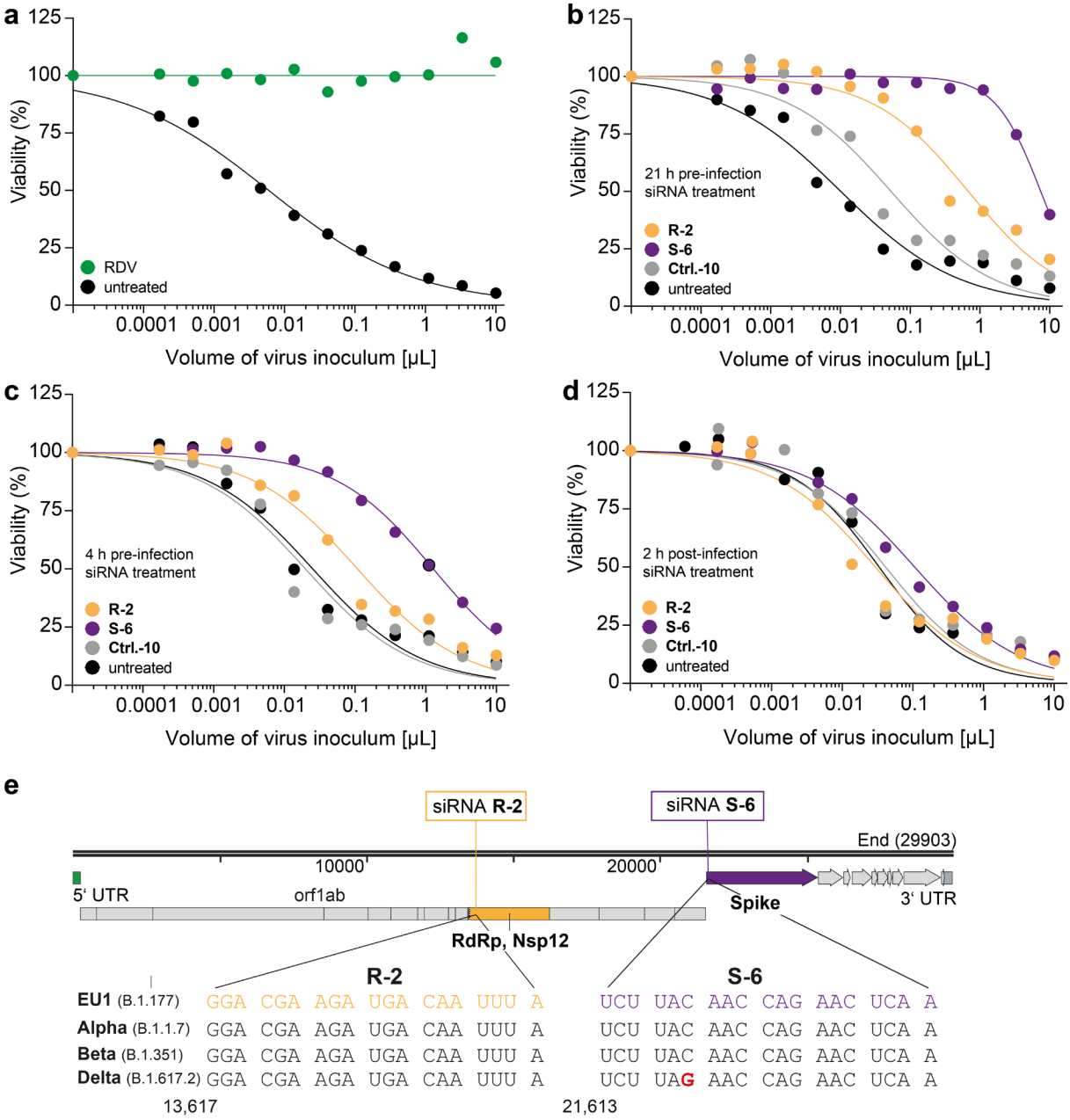

Figure S2: SARS-CoV-2 cytotoxicity assay including time-of-addition experiments and siRNA target sequences in VoCs Alpha, Beta and Delta. (a) Viability of MDA-MB-231-hACE2 cells depends on the SARS-CoV-2 virus inoculum (variant B.1.177 (EU1)) and specific treatment. Dots show the mean of two technical replicates from one representative biologically independent experiment. Treatment with 1 µM RDV 2 h pre-infection. (b – d) Time-of-addition experiments. Viability of MDA-MB-231-hACE2 cells depends on the SARS-CoV-2 virus inoculum (variant B.1.177 (EU1)) and specific treatment. Dots show the mean of technical replicates from one representative biologically independent experiment. siRNA treatment (20 nM, lipofection) 21 h pre-infection (b), 4 h pre-infection (c), or 2 h post-infection (**d**). (e) Target sequences of **R-2** and **S-6** aligned with the corresponding sequences in the VoCs B.1.1.7 (Alpha), B.1.351 (Beta) and B.1.617.2 (Delta) showing that these regions are not affected by mutations in Alpha and Beta, whereas there is a mismatch in the **S-6** target region at position 21,618 in the Delta variant.

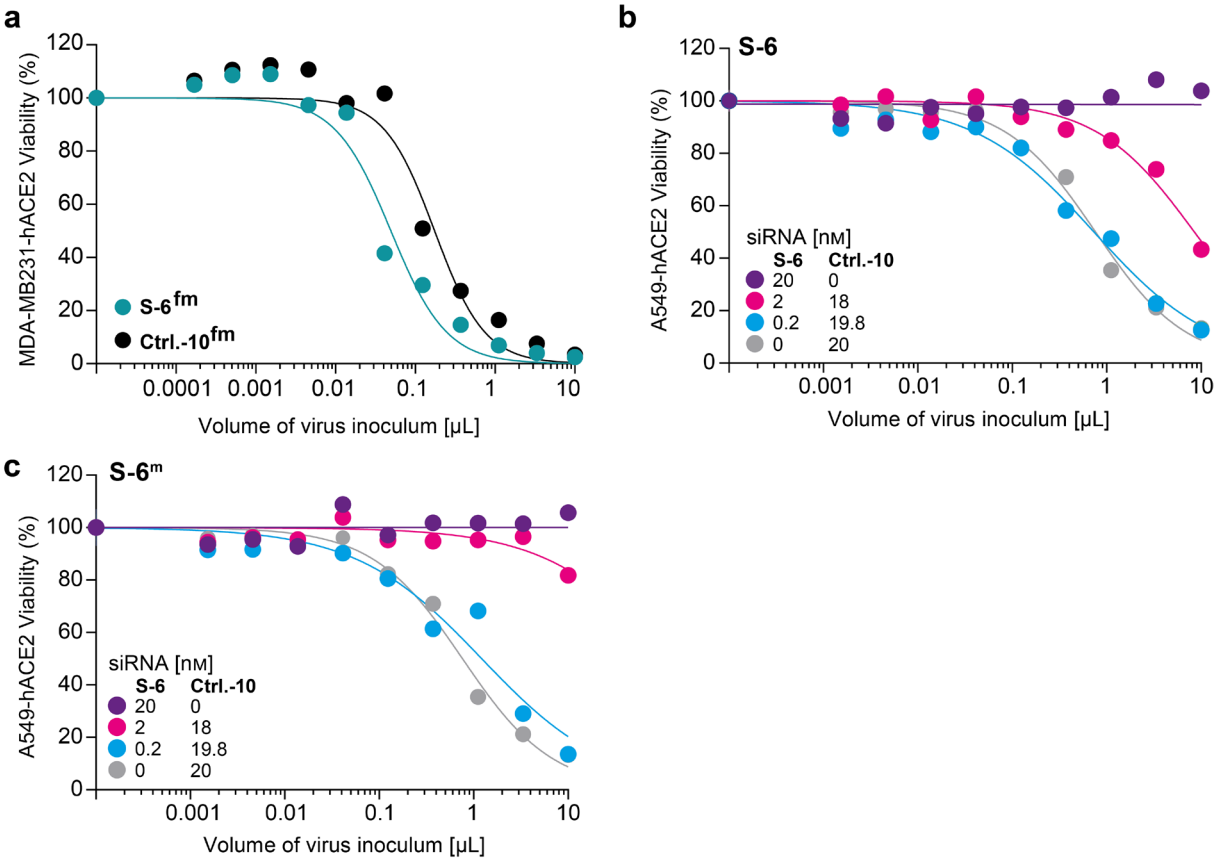

Figure S3: SARS-CoV-2 cytotoxicity assay with chemically modified siRNA. (a) Viability of MDA-MB-231-hACE2 with increasing SARS-CoV-2 virus inoculum (variant B.1.177 (EU1)) when treated with 40 nM **S-6^{fm}** using lipofection. Dots represent mean of two technical replicates. (b, c) Viability of SARS-CoV-2-infected A549-hACE2 cells in the context of titration of virus inoculum (0.0001 to 10 µL) and of **S-6** (b) or **S-6^{m}** (c) concentrations (0.2 to 20 nM, lipofection). Dots represent mean of two technical replicates. Representative data of one out of two independent experiments are displayed.

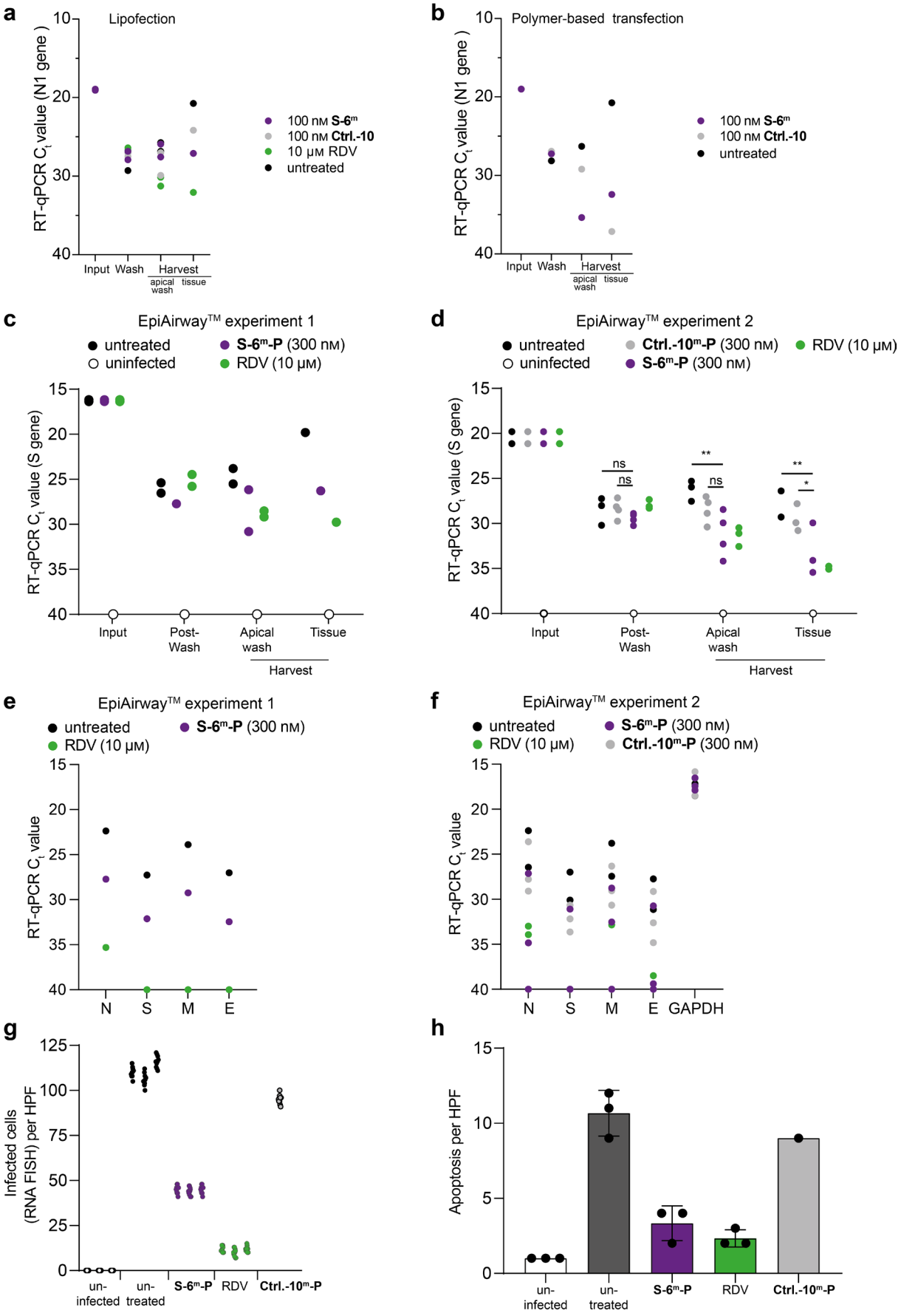

Figure S4: siRNA activity against SARS-CoV-2 infection of human 3D lung microtissues. (a, b) C_t values of SARS-CoV-2 RT-qPCR in 3D lung microtissues 72 h after virus challenge (SARS-CoV-2 variant B.1.177 (EU1)) are shown. Tissues were treated as indicated. (c, d) SARS-CoV-2 RT-qPCR results (C_t values depicted) of two independent SARS-CoV-2-infected (variant B.1.177

(EU1)) 3D lung microtissue experiments. C_t values for the viral inoculum (Input), the post apical wash (Post-wash) and the apical wash and tissue at harvest 72 h p.i. are shown. Each dot represents data from one independent well. Figure 3c shows the mean of all data depicted in Figure S4c, d for **S-6^m-P**, RDV and untreated control. No transfection reagent was used. (c) Activity of **S-6^m-P** (300 nM, 21 h pre-infection treatment) was tested compared to the untreated and the RDV (10 µM, 2 h pre-infection treatment) controls. (d) Activity of **S-6^m-P** (300 nM, 21 h pre-infection treatment) was tested against the **Ctrl.-10^m-P** (300 nM, 21 h pre-infection treatment), untreated and RDV (10 µM, 2 h pre-infection treatment) controls. Ordinary two-way ANOVA combined with Tukey's multiple comparisons test was performed. Details about the statistical analysis are given in the materials and methods section. (e, f) SARS-CoV-2 RT-qPCR results (C_t values depicted) of two independent SARS-CoV-2-infected (variant B.1.177 (EU1)) 3D lung microtissue experiments. C_t values for the viral sgmRNAs in the tissue harvest 72 h p.i. are shown. Each dot represents data from one independent well. Figure 3d shows the mean of all data depicted in Figure S3c, d for **S-6^m-P**, RDV and untreated control. No transfection reagent was used. (e) Activity of **S-6^m-P** (300 nM, 21 h pre-infection treatment) was tested compared to the untreated and the RDV (10 µM, 2 h pre-infection treatment) controls. (f) Activity of **S-6^m-P** (300 nM, 21 h pre-infection treatment) was tested against the **Ctrl.-10^m-P** (300 nM, 21 h pre-infection treatment), untreated and RDV (10 µM, 2 h pre-infection treatment) controls. (g) Quantitative SARS-CoV-2 RNA FISH analysis of 3D lung microtissues following SARS-CoV-2 infection (variant B.1.177 (EU1)). Each group represents data from ten HPFs from one independent experiment. (h) Histopathological analysis of uninfected and **S-6^m-P-**, **Ctrl.-10^m-P-**, RDV-pre-treated or untreated 3D lung microtissues 72 h post SARS-CoV-2 infection (variant B.1.177 (EU1)) to quantify apoptosis of epithelial cells. Bar represents mean, error bars represent SD.

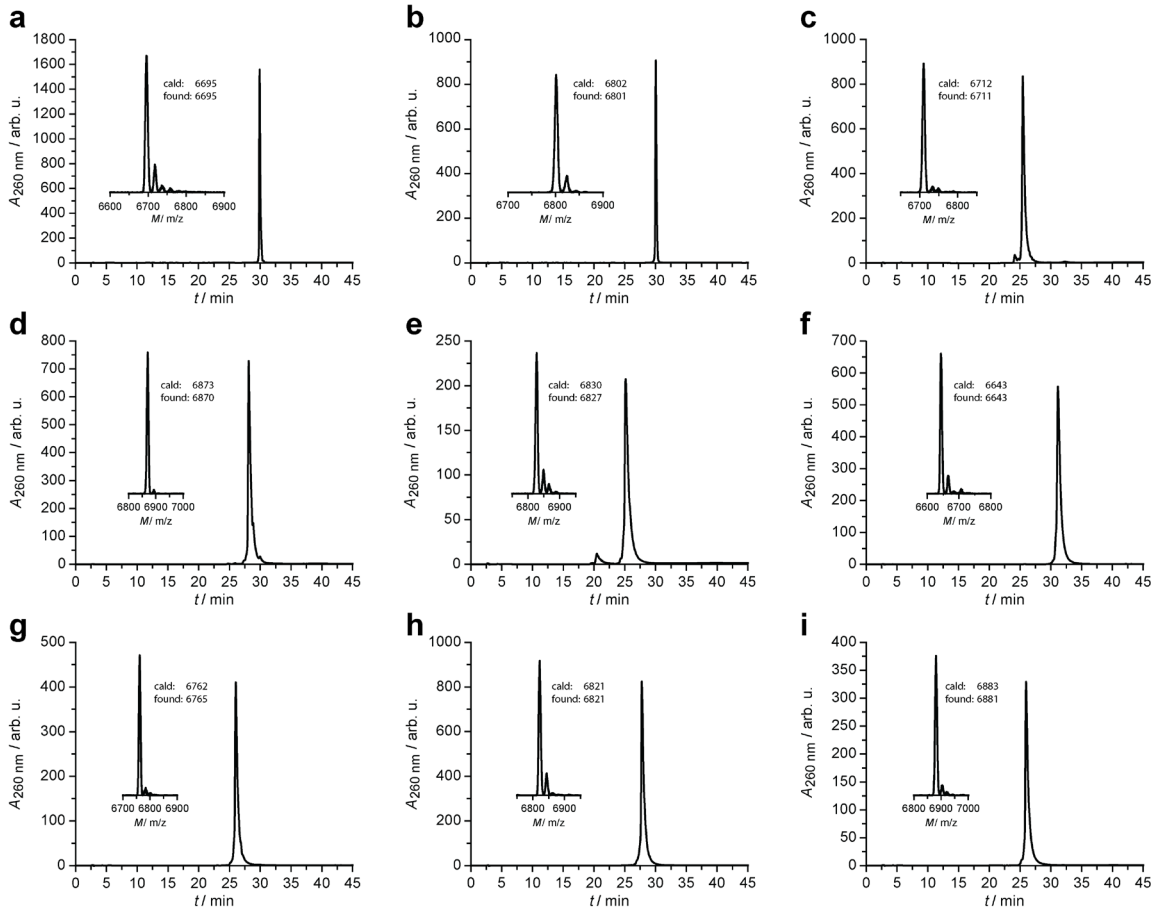

Figure S5: Analytical HPL-Chromatograms of the purified strands and the corresponding MALDI-TOF analysis. (a) **S-6^m-T*** sense (b) **S-6^m-T*** antisense (c) **S-6^m** antisense (d) **S-6^{fm}-T*** sense (e) **S-6^{fm}** antisense (f) **Ctrl.-10^m-T*** sense (g) **Ctrl.-10^m** antisense (h) **Ctrl.-10^{fm}-T*** sense (i) **Ctrl.-10^{fm}** antisense.

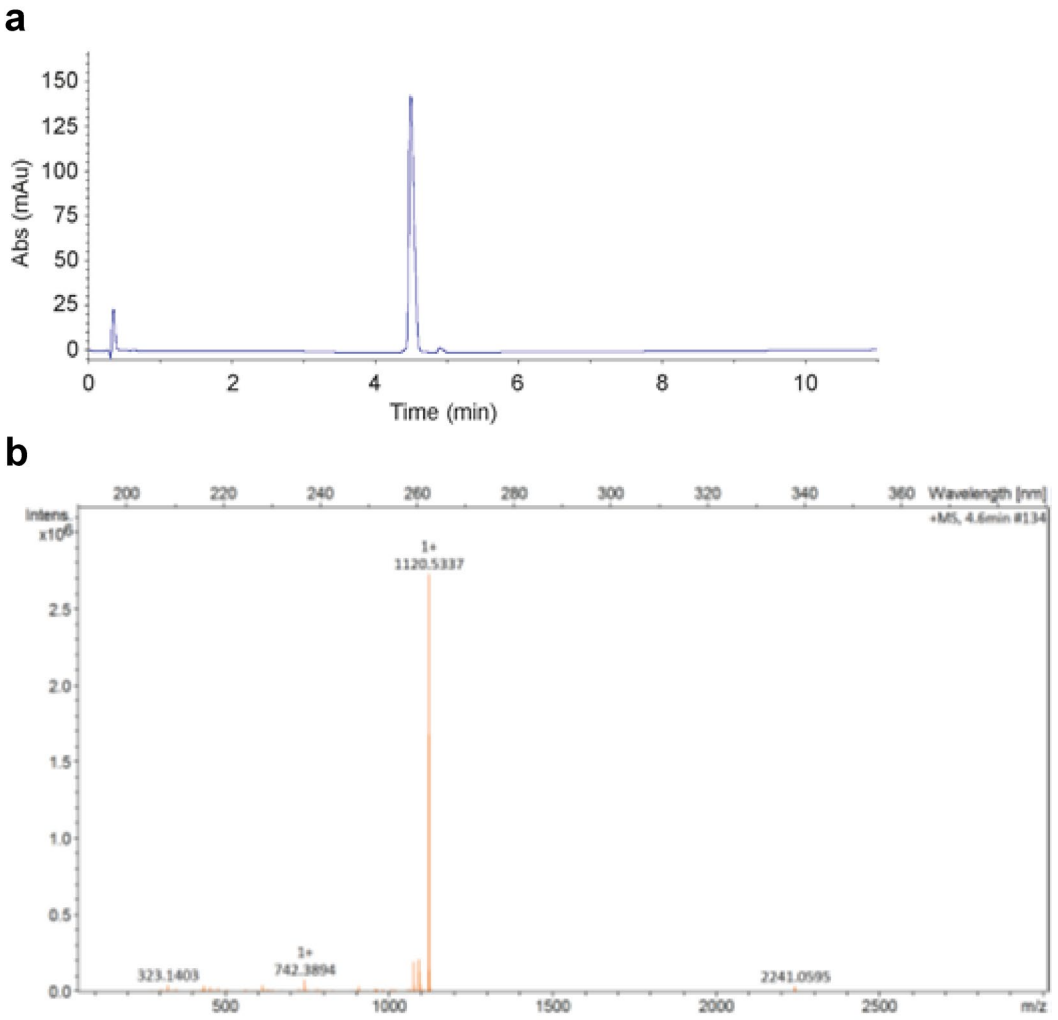

Figure S6: Purification of peptide P (N3-Deg3-CO-Tyr-Lys-Tyr-Arg-Tyr-Leu-OH). **(a)** HPL-Chromatograms of N3-Deg3-CO-Tyr-Lys-Tyr-Arg-Tyr-Leu-OH with a gradient of 40-100% of buffer **b** in 10 min. (b) ESI-MS data of N3-Deg3-CO-Tyr-Lys-Tyr-Arg-Tyr-Leu-OH.

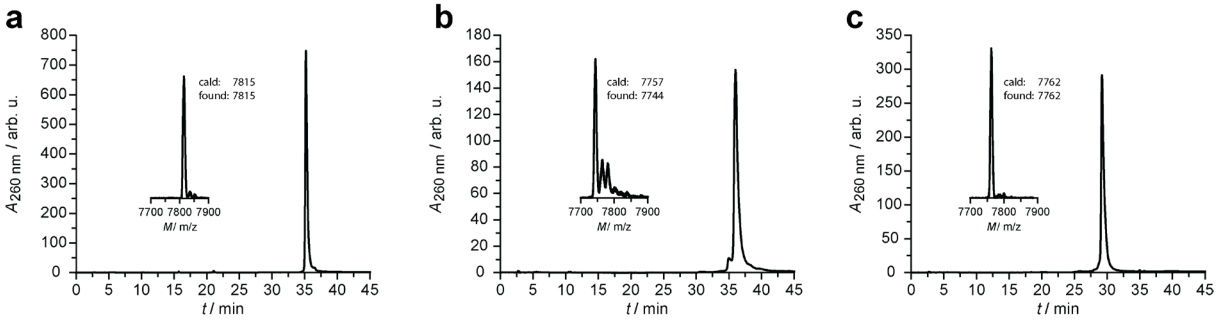

Figure S7: Analytical HPL-chromatograms of the purified click products as well as MALDI-TOF analysis. (a) **S-6^{m}-P** sense. (b) **S-6^{m}-Alexa647** antisense. (c) **Ctrl.-10^{m}-P** sense.

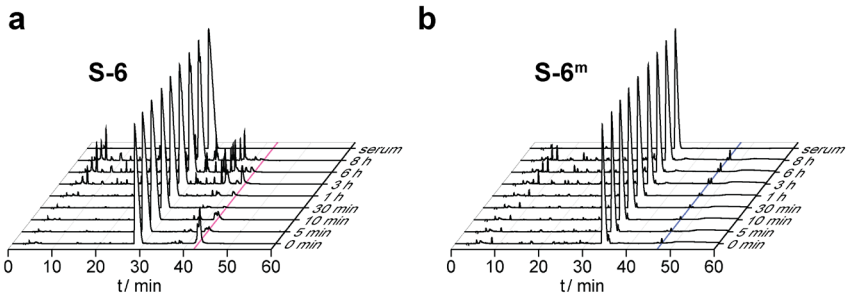

Figure S8: HPL-chromatograms of serum stability assay. (a) Serum stability assay of **S-6**. The magenta-coloured line indicates the signal of the siRNA. This area is shown in more detail in Figure 2b. (b) Serum stability assay of **S-6^{m}**. The blue-coloured line indicates the signal of the siRNA. This area is shown in more detail in Figure 2c.

Supporting Tables

Table S1: siRNA sequences of unmodified SARS-CoV-2 targeting siRNAs and the scrambled (non-targeting) siRNA.

siRNA	Viral RNA sequence target	Sequence (5' → 3')
L-1 sense	Leader	CCA ACC AAC UUU CGA UCU CTT
L-1 antisense		GAG AUC GAA AGU UGG UUG GTT
R-2 sense	RdRp, Nsp12	GGA CGA AGA UGA CAA UUU ATT
R-2 antisense		UAA AUU GUC AUC UUC GUC CTT
R-3 sense	RdRp, Nsp12	CAU GAA GAA ACA AUU UAU ATT
R-3 antisense		UAU AAA UUG UUU CUU CAU GTT
R-4 sense	RdRp, Nsp12	GGA AGG AAG UUC UGU UGA ATT
R-4 antisense		UUC AAC AGA ACU UCC UUC CTT
R-5 sense	RdRp, Nsp12	ACA GAU GGU ACA CUU AUG ATT
R-5 antisense		UCA UAA GUG UAC CAU CUG UTT
S-6 sense	Spike protein	UCU UAC AAC CAG AAC UCA ATT
S-6 antisense		UUG AGU UCU GGU UGU AAG ATT
S-7 sense	Spike protein	UUA CCC CCU GCA UAC ACU ATT
S-7 antisense		UAG UGU AUG CAG GGG GUA ATT
S-8 sense	Spike protein	CUC AAU UAC CCC CUG CAU ATT
S-8 antisense		UAU GCA GGG GGU AAU UGA GTT
S-9 sense	Spike protein	CUC AGG ACU UGU UCU UAC CTT
S-9 antisense		GGU AAG AAC AAG UCC UGA GTT
Ctrl.-10 sense	Non-targeting (scrambled)	ACU UAC UUG CAU CGU UCA UTT
Ctrl.-10 antisense		AUG AAC GAU GCA AGU AAG UTT

Table S2: Overview of the reporter plasmids for the dual-luciferase assay to screen the siRNA efficiencies. The listed inserted sequences are fused to the *Renilla* luciferase and the parts that are targeted by the siRNAs are marked in blue.

Plasmid name	Targeted by siRNA	Inserted sequence (5' → 3')	Viral sequence context Y/N?
A1	**L-1**	GTTCTTTAAGGTTTATACCTTCCCAGGTAACAAACCAACCAACTTTCG ATCTCTTGTAGATCTGTTCTCTAA	N
A2	**R-2**, **R-3**, **S-7**, **S-8**, **S-9**	GTCAGCTGATGCACAATCGTTTTTAAACGGGTTTGCGGTGTAAGTGCA GCCCGTCTTACACCGTGCGGCACAGGCACTAGTACTGATGTCGTATA CAGGGCTTTTGACATCTACAATGATAAAGTAGCTGGTTTTGCTAAATT CCTAAAAACTAATTGTTGTCGCTTCCAAGAAAAGGACGAAGATGACAA TTTAATTGATTCTTACTTTGTAGTTAAGAGACACACTTTCTCTAACTAC CAACATGAAGAAACAATTTATAATTTACTTAAGGATTGTCCAGCTGTTG CTAAACATGACTTCTTTAAGTTTAGAATAGACGGTGACATGGTACCAC ATATATCACGT|CTTGTTAACAACTAAACGAACAATGTTTGTTTTTCTTG TTTTATTGCCACTAGTCTCTAGTCAGTGTGTTAATCTTACAACCAGAAC TCAATTACCCCCTGCATACACTAATTCTTTCACACGTGGTGTTTATTAC CCTGACAAAGTTTTCAGATCCTCAGTTTTACATTCAACTCAGGACTTGT TCTTACCTTTCTTTTCCAATGTTACTTGGTTCCATGCTATACATGTCTC TGGGACCAATGGTACTAAGAGGTTTGATAACCCTGTCCTACCATTTAA TGATGGTGTTTATTTTGCTTCCACTGAGAAGTCTAACATAATAAGAGG CTGGATTTTTGGTACTACTTTAGATTCGAAGACCCAGTCCCTACTTATT GTTAATAACGCTACTAATGTTGTTATTAAAGTCTGTGAATTTCAATTTT GTAATGATCCATTTTTGGGTGTTTATTACCACAAAAACAACAAAAGTTG GAT	Y
A3	**R-4**, **R-5**, **S-6**	AAGGAAGGAAGTTCTGTTGAATTAAACAGATGGTACACTTATGATTAA TCTTACAACCAGAACTCAATTAACTCAGGACTTGTTCTTACCTT	N

Table S3: Details about the calculation of the CV50 values in Figure 1f - i. CV50 corresponds to the IC50 value. “n.a.” refers to cases, where the CV50 and the 95% confidence interval (CI) could not be determined unambiguously as the cytotoxicity was too low with the applied volumes of virus inoculum. siRNAs were applied with 40 nM total concentration, 21 h prior to virus challenge.

	S-6	R-2	S-6 + R-2	Ctrl.-10
EU1 (B.1.177)				
Best-fit values				
HillSlope	0.8896	1.042	n.a.	0.4227
CV50	8.063	3.329	n.a.	0.007258
Log(CV50)	0.9065	0.5223	n.a.	-2.139
Std. Error				
HillSlope	0.1324	0.1044	n.a.	0.04065
CV50	1.273	0.3202	n.a.	0.001677
95% CI (profile likelihood)				
HillSlope	0.6576 to 1.216	0.8619 to 1.271	n.a.	0.3463 to 0.5200
CV50	6.044 to 11.88	2.725 to 4.114	n.a.	0.00447 to 0.01168
Log(CV50)	0.7813 to 1.075	0.4353 to 0.6142	n.a.	-2.350 to -1.933
Goodness of Fit				
Degrees of Freedom	22	22	n.a.	22
R squared	0.8910	0.9596	n.a.	0.9396
Sum of Squares	795.6	596.4	n.a.	1423
Sy.x	6.014	5.207	n.a.	8.044
Constraints				
CV50	CV50 > 0	CV50 > 0	CV50 > 0	CV > 50
Number of points				
# of X values	24	24	24	24
# Y values analysed	24	24	24	24
Alpha VOC (B.1.1.7)				
Best-fit values				
HillSlope	n.a.	1.728	n.a.	0.7856
CV50	n.a.	12.49	n.a.	0.1598
Log(CV50)	n.a.	1.097	n.a.	-0.7963
Std. Error				
HillSlope	n.a.	0.3829	n.a.	0.07238
CV50	n.a.	1.393	n.a.	0.02105
95% CI (profile likelihood)				
HillSlope	n.a.	1.100 to 3.683	n.a.	0.6451 to 0.9767
CV50	n.a.	10.41 to 17.49	n.a.	0.1216 to 0.2117
Log(CV50)	n.a.	1.018 to 1.243	n.a.	-0.9149 to -0.6744
Goodness of Fit				
Degrees of Freedom	n.a.	22	n.a.	22
R squared	n.a.	0.8574	n.a.	0.9705
Sum of Squares	n.a.	554.6	n.a.	908.0
Sy.x	n.a.	5.021	n.a.	6.424
Constraints				
CV50	CV50 > 0	CV50 > 0	CV50 > 0	CV > 50
Number of points				
# of X values	24	24	24	24
# Y values analysed	24	24	24	24
Beta VOC (B.1.351)				
Best-fit values				
HillSlope	1.335	1.051	n.a.	0.5809
CV50	12.53	3.190	n.a.	0.01571
Log(CV50)	1.098	0.5038	n.a.	-1.804
Std. Error				
HillSlope	0.2804	0.08898	n.a.	0.04608
CV50	1.882	0.2591	n.a.	0.002358
95% CI (profile likelihood)				
HillSlope	0.9158 to 1.991	0.8953 to 1.238	n.a.	0.4898 to 0.6979
CV50	9.809 to 18.71	2.689 to 3.815	n.a.	0.01152 to 0.02152
Log(CV50)	0.9916 to 1.272	0.4296 to 0.5815	n.a.	-1.938 to -1.667
Goodness of Fit				
Degrees of Freedom	22	22	n.a.	22
R squared	0.8290	0.9699	n.a.	0.9710
Sum of Squares	718.1	432.3	n.a.	867.1

Sy.x	5.713	4.433	n.a.	6.278
Constraints				
CV50	CV50 > 0	CV50 > 0	CV50 > 0	CV > 50
Number of points				
# of X values	24	24	24	24
# Y values analysed	24	24	24	24

Delta VOC (B.1.617.2)	**S-6**	**S-6 + R-2**	**S-6δ**	**Ctrl.-10**
Best-fit values				
HillSlope	0.6885	0.8244	1.285	0.6749
CV50	0.4374	3.435	9.555	0.03284
Log(CV50)	-0.3591	0.5359	0.9802	-1.484
Std. Error				
HillSlope	0.0369	0.09183	0.1535	0.05481
CV50	0.05336	0.4456	0.8109	0.004436
95% CI (profile likelihood)				
HillSlope	0.5919 to 0.8056	0.6729 to 1.011	0.9937 to 1.657	0.5673 to 0.8173
CV50	0.3383 to 0.5693	2.625 to 4.613	8.136 to 11.75	0.02482 to 0.04374
Log(CV50)	-0.4707 to -0.2447	0.4192 to 0.6639	0.9104 to 1.070	-1.605 to -1.359
Goodness of Fit				
Degrees of Freedom	22	22	22	22
R squared	0.9733	0.9386	0.9310	0.9750
Sum of Squares	672.8	776.4	363.7	820.6
Sy.x	5.530	5.941	4.066	6.107
Constraints				
CV50	CV50 > 0	CV50 > 0	CV50 > 0	CV > 50
Number of points				
# of X values	24	24	24	24
# Y values analysed	24	24	24	24

Table S4: Details about the calculation of the CV50 values in Figure 2e, f. CV50 corresponds to the IC50 value. A = 20 nM **S-6** or **S-6^m** + 0 nM **Ctrl.-10**, B = 2 nM **S-6** or **S-6^m** + 18 nM **Ctrl.-10**, C = 0.2 nM **S-6** or **S-6^m** + 19.8 nM **Ctrl.-10**, D = 0.02 nM **S-6** or **S-6^m** + 19.98 nM **Ctrl.-10**, E = 0 nM **S-6** or **S-6^m** + 20 nM **Ctrl.-10**.

	A	B	C	D	E
S-6^m treatment					
Best-fit values					
HillSlope	0.9282	0.8438	0.4413	0.3480	0.3159
CV50	15.14	9.876	0.1939	0.001238	0.005409
Log(CV50)	1.180	0.9946	-0.7125	-1.907	-2.267
Std. Error					
HillSlope	0.1201	0.07660	0.02208	0.01683	0.01982
CV50	2.280	1.037	0.02219	0.001647	0.0009914
95% CI (profile likelihood)					
HillSlope	0.7041 to 1.213	0.6881 to 1.031	0.3995 to 0.4877	0.3155 to 0.3839	0.2781 to 0.3583
CV50	11.66 to 22.51	8.100 to 12.76	0.1529 to 0.2465	0.009386 to 0.01630	0.003696 to 0.007863
Log(CV50)	1.067 to 1.352	0.9085 to 1.106	-0.8156 to -0.6081	-2.028 to -1.788	-2.432 to -2.104
Goodness of Fit					
Degrees of Freedom	22	22	22	22	22
R squared	0.9000	0.9492	0.9826	0.9800	0.9636
Sum of Squares	311.0	256.6	366.5	380.6	609.2
Sy.x	3.760	3.415	4.082	4.159	5.262
Constraints					
CV50	CV50 > 0	CV50 > 0	CV50 > 0	CV > 50	CV > 50
Number of points					
# of X values	24	24	24	24	24
# Y values analysed	24	24	24	24	24
S-6 treatment					
Best-fit values					
HillSlope	1.120.	0.9597	0.3640	0.3199	0.3159
CV50	9.896	5.532	0.02813	0.007129	0.005409
Log(CV50)	0.9955	0.7429	-1.551	-2.147	-2.267
Std. Error					
HillSlope	0.1414	0.08769	0.01870	0.01681	0.01982
CV50	1.046	0.4945	0.003867	0.001084	0.0009914
95% CI (profile likelihood)					
HillSlope	0.8582 to 1.446	0.7985 to 1.153	0.3285 to 0.4032	0.2877 to 0.3554	0.2781 to 0.3583
CV50	8.131 to 12.89	4.626 to 6.747	0.02112 to 0.03746	0.005194 to 0.009744	0.003696 to 0.007863
Log(CV50)	0.9101 to 1.110	0.6652 to 0.8291	-1.675 to -1.426	-2.285 to -2.011	-2.432 to -2.104
Goodness of Fit					
Degrees of Freedom	22	22	22	22	22
R squared	0.9091	0.9571	0.9785	0.9745	0.9636
Sum of Squares	418.5	386.8	436.1	434.8	609.2
Sy.x	4.361	4.193	4.452	4.446	5.262
Constraints					
CV50	CV50 > 0	CV50 > 0	CV50 > 0	CV > 50	CV > 50
Number of points					
# of X values	24	24	24	24	24
# Y values analysed	24	24	24	24	24

Table S5: **Summary of synthesized RNA strands**. X = C8-Alkyne-dU, A_m = 2'-OMe-A, C_m = 2'-OMe-C, G_m = 2'-OMe-G, U_m = 2'-OMe-U, A_F = 2'-F-A, C_F = 2'-F-C, G_F = 2'-F-G, U_F = 2'-F-U.

siRNA	Sequence 5' → 3'
S-6^m sense	UCU UAC$_m$ AAC CAG AAC UC$_m$A ATT
S-6^m sense (alkyne)	UCU UAC$_m$ AAC CAG AAC UC$_m$A AXT
S-6^m antisense	UUG AGU$_m$ UCU GGU UGU$_m$ AAG ATT
S-6^m antisense (alkyne)	UUG AGU$_m$ UCU GGU UGU$_m$ AAG AXT
S-6^{fm} sense (alkyne)	$U_mC_mU_m$ $U_mA_mC_m$ $A_FA_mC_F$ $C_mA_FG_m$ $A_FA_mC_F$ $U_mC_mA_m$ A_mXT
S-6^{fm} antisense	$U_mU_FG_F$ $A_FG_mU_F$ $U_mC_FU_m$ $G_FG_mU_F$ $U_mG_FU_m$ $A_FA_mG_F$ A_mTT
Ctrl.-10^m sense (alkyne)	ACU UAC$_m$ UUG CAU CGU UC$_m$A UXT
Ctrl.-10^m antisense	AUG AAC$_m$ GAU GCA AGU$_m$ AAG UTT
Ctrl.-10^{fm} sense (alkyne)	$A_mC_mU_m$ $U_mA_mC_m$ $U_FU_mG_F$ $C_mA_FU_m$ $C_FG_mU_F$ $U_mC_mA_m$ U_mXT
Ctrl.-10^{fm} antisense	$A_mU_FG_F$ $A_FA_mC_F$ $G_mA_FU_m$ $G_FC_mA_F$ $A_mG_FU_m$ $A_FA_mG_F$ U_mTT

Table S6: Summary of clicked RNA strands and their HPLC gradients. X = C8-Alkyne-dU, C_m = 2'-OMe-C, U_m = 2'-OMe-U.

RNA	Sequence 5' → 3'	HPLC gradient
S-6^m-P sense	UCU UAC$_m$ AAC CAG AAC UC$_m$A A(X-YKYRYL)T	0_35
S-6^m-Alexa647 antisense	UUG AGU$_m$ UCU GGU UGU$_m$ AAG A(X-Alexa647)T	0_30
Ctrl.-10^m-P sense	ACU UAC$_m$ UUG CAU CGU UC$_m$A U(X-YKYRYL)T	0_40

Table S7: List of primers for RT-qPCR. fw = forward, rev = reverse.

Primer name	Sequence (5' → 3')	Application	Reference
Spike-total_fw	GCT GGT GCT GCA GCT TAT TA	RT-qPCR (iTaq SYBR Green); viral genome and sgmRNA	[6]
Spike-total_rev	AGG GTC AAG TGC ACA GTC TA		
Leader_fw_sgmRNA	CCT TCC CAG GTA ACA AAC CAA CC	RT-qPCR (PowerUp SYBR Green); sgmRNAs	
M_rev_sgmRNA	GGT AAT AGT ACC GTT GGA ATC TGC C		
N_rev_sgmRNA	GGG TGC ATT TCG CTG ATT TTG G		
E_rev_sgmRNA	CCT GTC TCT TCC GAA ACG AAT GAG		
S_rev_sgmRNA	ACA CAC TGA CTA GAG ACT AGT GGC		
GAPDH_fw	ACC ACA GTC CAT GCC ATC AC	RT-qPCR (PowerUp SYBR Green); human reference gene	
GAPDH_rev	TCC ACC ACC CTG TTG CTG TA		

References Supplementary Information

[1] a) P. R. Wratil, N. A. Schmacke, A. Osterman, T. Weinberger, J. Rech, B. Karakoc, M. Zeilberger, J. Steffen, T. T. Mueller, P. M. Spaeth, M. Stern, M. Albanese, H. Thun, J. Reinbold, B. Sandmeyer, P. Kressirer, B. Grabein, P. Falkai, K. Adorjan, V. Hornung, L. Kaderali, M. Klein, O. T. Keppler, *Infection* **2022**, *50*, 381-394; b) M. Muenchhoff, A. Graf, S. Krebs, C. Quartucci, S. Hasmann, J. C. Hellmuth, C. Scherer, A. Osterman, S. Boehm, C. Mandel, A. S. Becker-Pennrich, M. Zoller, H. C. Stubbe, S. Munker, D. Munker, K. Milger, M. Gapp, S. Schneider, A. Ruhle, L. Jocham, L. Nicolai, K. Pekayvaz, T. Weinberger, H. Mairhofer, E. Khatamzas, K. Hofmann, P. M. Spaeth, S. Bender, S. Kääb, B. Zwissler, J. Mayerle, J. Behr, M. von Bergwelt-Baildon, M. Reincke, B. Grabein, C. L. Hinske, H. Blum, O. T. Keppler, *Euro. Surveill.* **2021**, *26*, 2002066; c) P. R. Wratil, M. Stern, A. Priller, A. Willmann, G. Almanzar, E. Vogel, M. Feuerherd, C. C. Cheng, S. Yazici, C. Christa, S. Jeske, G. Lupoli, T. Vogt, M. Albanese, E. Mejías-Pérez, S. Bauernfried, N. Graf, H. Mijocevic, M. Vu, K. Tinnefeld, J. Wettengel, D. Hoffmann, M. Muenchhoff, C. Daechert, H. Mairhofer, S. Krebs, V. Fingerle, A. Graf, P. Steininger, H. Blum, V. Hornung, B. Liebl, K. Überla, M. Prelog, P. Knolle, O. T. Keppler, U. Protzer, *Nat. Med.* **2022**, *28*, 496-503.

[2] M. Muenchhoff, H. Mairhofer, H. Nitschko, N. Grzimek-Koschewa, D. Hoffmann, A. Berger, H. Rabenau, M. Widera, N. Ackermann, R. Konrad, S. Zange, A. Graf, S. Krebs, H. Blum, A. Sing, B. Liebl, R. Wölfel, S. Ciesek, C. Drosten, U. Protzer, S. Boehm, O. T. Keppler, *Euro Surveill.* **2020**, *25*, 2001057.

[3] J. R. Tyson, P. James, D. Stoddart, N. Sparks, A. Wickenhagen, G. Hall, J. H. Choi, H. Lapointe, K. Kamelian, A. D. Smith, N. Prystajecky, I. Goodfellow, S. J. Wilson, R. Harrigan, T. P. Snutch, N. J. Loman, J. Quick, *bioRxiv* **2020**, 2020.09.04.283077.

[4] T. Weinberger, J. Steffen, A. Osterman, T. T. Mueller, M. Muenchhoff, P. R. Wratil, A. Graf, S. Krebs, C. Quartucci, P. M. Spaeth, B. Grabein, K. Adorjan, H. Blum, O. T. Keppler, M. Klein, *Clin. Infect. Dis.* **2021**.

[5] P.-A. Koenig, H. Das, H. Liu, B. M. Kümmerer, F. N. Gohr, L.-M. Jenster, L. D. J. Schiffelers, Y. M. Tesfamariam, M. Uchima, J. D. Wuerth, K. Gatterdam, N. Ruetalo, M. H. Christensen, C. I. Fandrey, S. Normann, J. M. P. Tödtmann, S. Pritzl, L. Hanke, J. Boos, M. Yuan, X. Zhu, J. L. Schmid-Burgk, H. Kato, M. Schindler, I. A. Wilson, M. Geyer, K. U. Ludwig, B. M. Hällberg, N. C. Wu, F. I. Schmidt, *Science* **2021**, *371*, eabe6230.

[6] M. Park, J. Won, B. Y. Choi, C. J. Lee, *Exp. Mol. Med.* **2020**, *52*, 963-977.